Check for updates

Seasonal constraints on the burial of organic carbon in the eutrophic Lake Taihu

Yanhong Xu, Yuxin He*, Jiali Pang and Yongge Sun

Organic Geochemistry Unit, Key Laboratory of Geoscience Big Data and Deep Resource of Zhejiang Province, School of Earth Sciences, Zhejiang University, Hangzhou, China

Eutrophication alters the function of lake ecosystems through phytoplankton blooms and is a major contributor to organic carbon (OC) burial in lakes worldwide. Although Lake Taihu is notable for its severe eutrophication yet low OC burial, why cyanobacteria-derived OC is ineffectively buried in the lake is unknown. Because seasonal hydrological and ecological dynamics in eutrophic lacustrine ecosystems would significantly modify the preservation and degradation behaviors of OC, seasonal variations in paired particulate samples from both the water column and surface sediment are critical in evaluating cyanobacteria-derived OC burial. In this study, we present the steroid results of water and sediments collected from Meiliang Bay in Lake Taihu across cyanobacteria-bloom and decay seasons (from May 2018 to June 2019) to investigate constraints on the seasonal burial of autochthonous and allochthonous OC. The results indicate that cyanobacteria contribute a considerable amount of OC to the water body in the cyanobacterial bloom season, while terrestrial OC becomes the main contributor during the cyanobacterial decay season. Although OC degradation occurs throughout the water column, substantially more OC degradation was observed at the water-sediment interface. The extensive degradation of OC in the bloom season eventually reverses the seasonal distribution characteristics of particulate OC in the water column, leading to less accumulation of OC under the background of higher cyanobacteria-derived OC input. The combined effect of OC bioavailability, temperature, oxygen exposure, and more importantly microorganism activities, accounts for much higher OC degradation rates in the bloom season. Similar phenomena were observed in subtropical shallow lakes with high primary productivity, suggesting that eutrophication might have a limited influence on OC burial when compared to other factors related to OC degradation.

KEYWORDS

Eutrophication1, sterols2, particulate organic carbon3, sedimentary organic carbon4, lake Taihu5, OC burial6

1 Introduction

Lakes are an important global carbon storage system due to their considerable organic carbon (OC) burial (Mendonça et al., 2017). The amount and source of the OC (Watanabe and Kuwae, 2015; Guillemette et al., 2017), oxygen concentration (Sobek et al., 2009; Wang et al., 2018), exposure time (Sobek et al., 2009), temperature (Gudasz et al., 2010; Cardoso et al., 2014), and microorganism activities (Tabuchi et al., 2010; Cai et al., 2014) have substantial influences on the OC sequestration function of lakes. Many lakes worldwide have been eutrophicated in recent decades as a result of global warming, increased atmospheric CO_2 concentrations, and increasing anthropogenic nutrient inputs (Wagner and Adrian, 2009; Kosten et al., 2012;

Przytulska et al., 2017; Salk et al., 2022). Eutrophication is usually characterized by a strong bloom of cyanobacteria (Huisman et al., 2018), which increases the amount of fresh OC available for subsequent depositional processes (Dong et al., 2012; Anderson et al., 2014; Xiao et al., 2020a). Eutrophication also promotes heterotrophic bacterial activity and, thus, mineralization of OC (Niu et al., 2011; Kiersztyn et al., 2019; Zhu et al., 2019). Temperature fluctuations may cause frequent phytoplankton blooms and recesses, resulting in seasonal variations in the amount and composition of OC input, as well as preservation and degradation behaviors in eutrophic lakes (McCullough et al., 2018). Therefore, it is crucial to determine the amount of cyanobacteria-derived OC that can be effectively preserved in the bloom and decay seasons.

Lake Taihu, a large shallow lake on the Yangtze floodplain, is characterized by cyanobacterial blooms (*Microcystis* blooms) due to rapid economic development and intensive usage of water resources (Qin et al., 2013). The western and northern parts of the lake are severely eutrophic regions, while the eastern bays are inhabited by dense aquatic vegetation. However, OC burial in the northern eutrophic area of Lake Taihu is only approximately 28 g C m^{-2} yr^{-1} in recent years (Gui et al., 2013), which is lower than that in other lakes with similar bioproduction or eutrophication levels (e.g., Lake Okeechobee, 60 g C m^{-2} yr^{-1}, Dong et al., 2012). Previous studies have demonstrated that the source of sedimentary organic matter contains a high proportion of terrestrial OC (Zhang et al., 2017a; Li et al., 2020; Zhang et al., 2021) in contrast to the high cyanobacterial input from surface waters in eutrophic regions (Xu et al., 2015a). As a result, Lake Taihu has exhibited remarkable decomposition of cyanobacteria-derived OC. Therefore, information on when and where these OC are degraded is important for exploring the potential effect of eutrophication on OC burial in Lake Taihu.

Autochthonous OC (synthesized by bacterial exudates and photosynthesis by primary producers) is primarily composed of proteins, peptides, amino acids, polysaccharides, oligosaccharides, lipids, and various organic acids that are easily oxidized and available to microorganisms (Li et al., 2012; Bai et al., 2017). In lakes, OC degradation mainly occurs during particle settlement, deposition through the water column (Li and Minor, 2015; Wang et al., 2018), surface of sediments, and following deeper sediments (Middelburg, 2018). During particle settlement through the water column, particulate OC (POC) can be directly oxidized or photodegraded (He et al., 2016). Additionally, a critical portion of POC can provide material and energy sources for heterotrophic bacteria (Tranvik et al., 2009), which further removes the phytoplankton bio-productivity accumulated at the water surface. Such OC degradation by heterotrophic bacteria can account for more than 90% of the primary bio-productivity in the case of lakes like Lake Superior (Li and Minor, 2015). The remaining POC that reaches the lake bottom is an important precursor of sedimentary OC (SOC) (Vachon et al., 2021). At the water-sediment interface, preferential utilization and degradation of labile OC proceed *via* anaerobic organism consumption (Meyers and Ishiwatari, 1993; Liu et al., 2022). In this sense, paired samples from POC through the water column and SOC in the surface sediments can address the exact preservation and degradation behaviors of autochthonous OC.

Steroids are a group of widely distributed biomarkers in aquatic ecosystems that are indicative of eukaryotes and possibly cyanobacteria (Volkman, 1986; 2005); consequently, they are suitable for investigating the transport and sinking of POC derived

from phytoplankton including cyanobacteria, some protists, and most single-celled plants (diatoms, dinoflagellates, green algae). For instance, cholesterol is usually recognized to originate from cyanobacteria and eukaryotic phytoplankton in lake systems (Meyers, 1997; Volkman, 2005) such as Lake Suwa in Japan (Nishimura and Koyama, 1977) and lakes in the middle and lower Yangtze River in China (Zhang et al., 2019). C$_{28}$ sterols, including brassicasterol and chalinasterol, have been widely utilized as indicators of diatom sources (Volkman, 2005; Köseoğlu et al., 2019); C$_{29}$ sterols are typically found in vascular plants and microalgae (Meyers, 1997; Volkman et al., 1998); C$_{30}$ sterol (dinosterol) is a specific biomarker for dinoflagellates (Robinson et al., 1984). 5α (H)-stanols are related to a bacterial reduction in unsaturated sterols (e.g., cholesterol and sitosterol), which can be used to evaluate OC biodegradation (Nishimura and Koyama, 1977; Mermoud et al., 1985) and lacustrine redox conditions (Nakakuni et al., 2018). Accordingly, sterols and stanols respond sensitively to source changes and are suitable for tracking seasonal variations in SOC and POC.
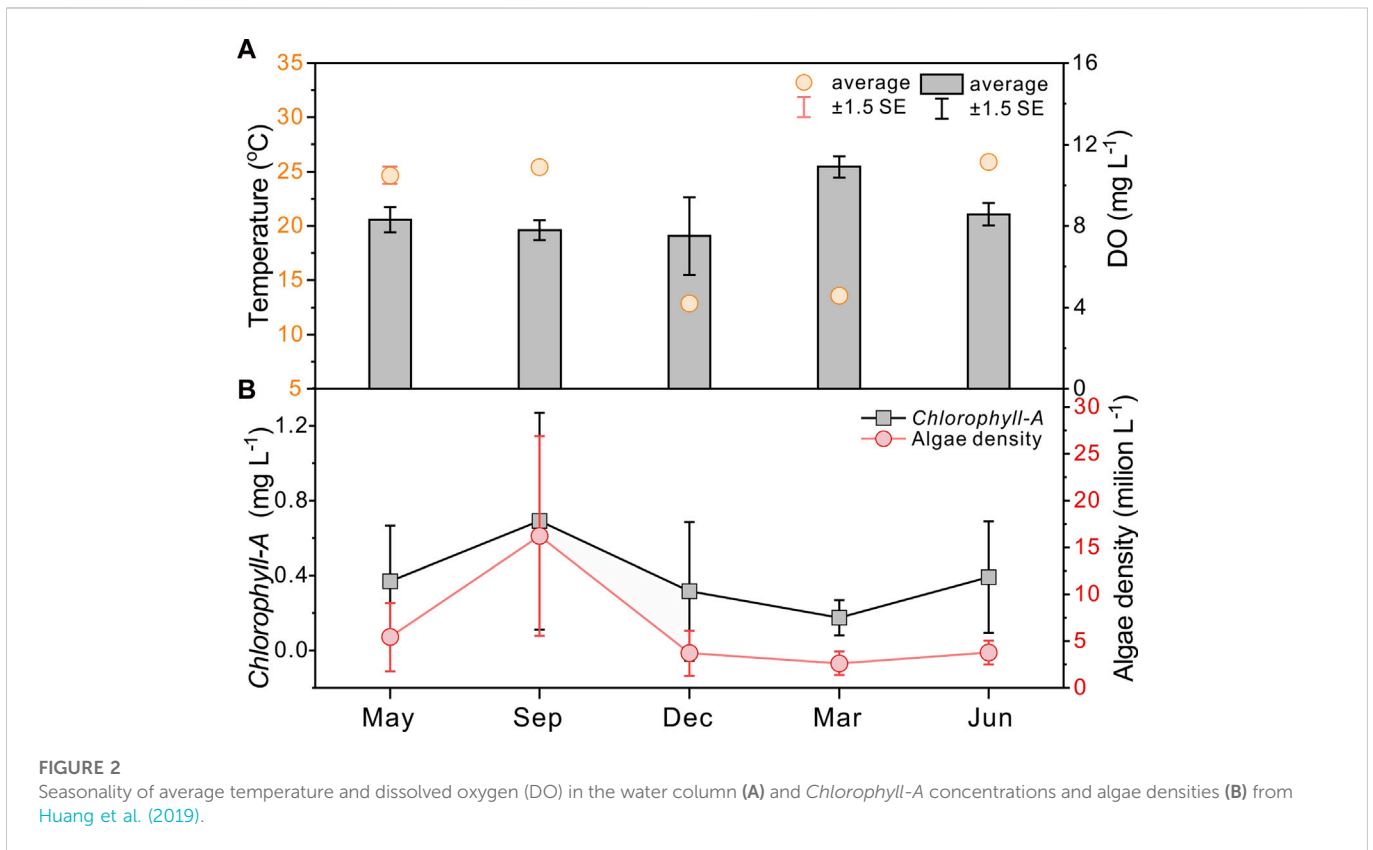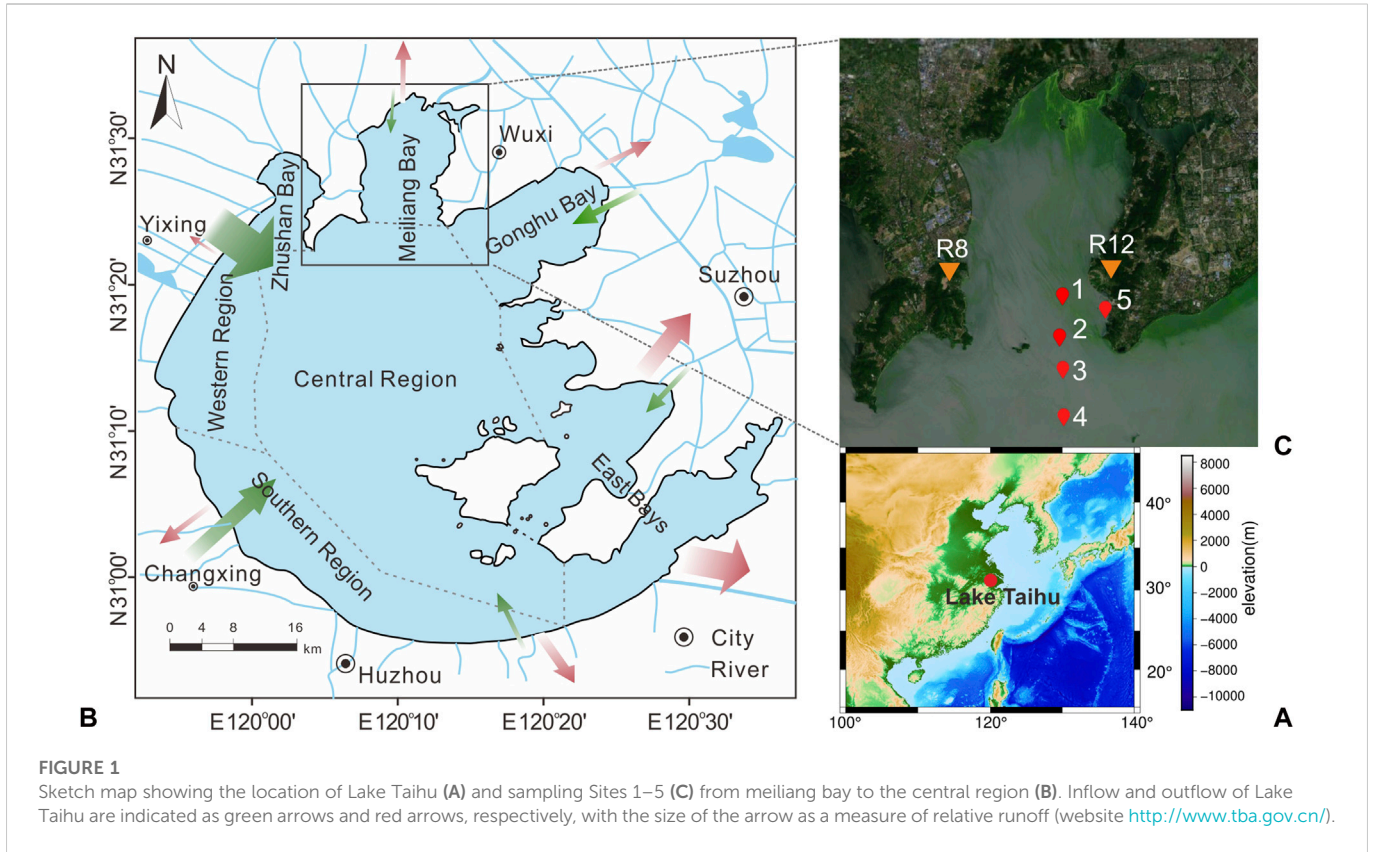
In this study, we present steroid results from water and sediments collected in Meiliang Bay, Lake Taihu, across cyanobacteria-bloom and decay seasons from an annual cycle (from May 2018 to June 2019). The main objectives of this study were to investigate the seasonal characteristics and sinking processes of POC and SOC to elucidate whether and why cyanobacteria-derived OC is ineffectively buried in Lake Taihu. The results would eventually address the potential effect of eutrophication on OC cycling in Lake Taihu.

2 Materials and methods

2.1 Study area and sample collection

Lake Taihu, the third largest freshwater lake in eastern China, has a surface area of about 2400 km^2, a catchment of 36,500 km^2, and an average depth of 1.9 m, respectively (Figure 1). The lake has a short water retention time of approximately 284 days due to an intensive river network with 172 rivers or channels connecting to the lake and large annual inflowing water input of 57 × 10^8 m^3 (Qin et al., 2007). Inflow rivers are located in the northern and western regions, whereas outflow rivers are in the eastern region. The spatial sewage input leads to the lake being divided into 3 different ecotypes based on eutrophic status and vegetation distribution (Xiao et al., 2020b; Zhang et al., 2021). The nutrient input from inflow rivers in Zhushan Bay, Meiliang Bay, and the western region has made these regions the most eutrophic parts of Lake Taihu.

In Lake Taihu, relatively warm temperatures prolong the cyanobacterial bloom period in a year, keeping high *Chlorophyll-A* concentrations and phytoplankton densities from May to November and low values from December to next April (Figure 2, data from Huang et al., 2019). Accordingly, water and sediment collections in Meiliang Bay were conducted from May 2018 to June 2019 (namely 05/2018, 09/2018, 12/2018, 03/2019, and 06/2019). According to the field observations and long-term monitoring records of lake *Chlorophyll-A* concentrations (Figure 2; Huang et al., 2019), sample dates of May 2018, September 2018, and June 2019 belong to the cyanobacterial bloom season, whereas December 2018 and March 2019 are the cyanobacterial decay season. Sampling sites include pelagic (sites 1–4) and shore areas (site 5), which are ideal areas for investigation of the frequent occurrence of cyanobacterial blooms

FIGURE 1
Sketch map showing the location of Lake Taihu **(A)** and sampling Sites 1–5 **(C)** from meiliang bay to the central region **(B)**. Inflow and outflow of Lake Taihu are indicated as green arrows and red arrows, respectively, with the size of the arrow as a measure of relative runoff (website http://www.tba.gov.cn/).

FIGURE 2
Seasonality of average temperature and dissolved oxygen (DO) in the water column **(A)** and *Chlorophyll-A* concentrations and algae densities **(B)** from Huang et al. (2019).

in Meiliang Bay (Figure 1). Water samples from the surface (top ~30 cm), middle, and bottom (~10 cm above water-sediment interface) layers were collected except for site 5 (only surface and bottom water). For the surface sediments, we only collected the top yellow-brown surface layers. Considering the high sedimentation rate in Meiliang Bay, these sediments should track the freshly deposited OC in recent months. Besides, water temperature (T) and dissolved oxygen (DO) were *in-situ* measured using Yellow Springs Instruments Professional Plus (YSI ProPlus). The particulate samples were extracted by pretreated 0.7 μm glass fiber filters in the field (Whatman GF/F, 4 h at 470°C). All particulate and sediment samples were immediately frozen at −20°C and brought back to the laboratory for further geochemical analysis. For the end member detection, the cyanobacteria sample aggregated in surface water and the water sample from rivers around Meiliang Bay were collected in September 2018 and September 2020, respectively (Figure 1).

2.2 Total organic carbon and stable carbon isotopic analyses

Before analysis of the total organic carbon content (TOC) and carbon isotopes ($\delta^{13}C$), the particulate and sediment samples were frozen-dried and added with the HCl solvent (6 N, 60°C for 2 h) to remove carbonates, followed by deionized water rinsing and drying. Thereafter, POC contents and sedimentary TOC contents were measured with a Euro Vector EA-3000 elemental analyzer (EA). The standard samples were run routinely to control the performance of the EA, and the uncertainty of the analysis was < ±0.03%. Carbon isotopes of POC ($\delta^{13}C_{POC}$) and sedimentary organic carbon ($\delta^{13}C_{SOC}$, VPDB standard) were determined by a Thermo Fisher FLASH2000 EA connected with MAT-253 Isotopic Ratio Mass Spectrometer (IRMS). Cellulose and caffeine with known $\delta^{13}C$ values were used to monitor the measurement. Two parallel analyses were conducted for each sample and the 1 σ precision of the replicate $\delta^{13}C_{org}$ analysis is < ±0.2‰.

2.3 Biomarker analysis

Biomarker extraction and purification of the surface and bottom lake water, cyanobacteria, and surface river water follow the procedure of Sun et al. (2019). Briefly, particles concentrated in 0.7 μm glass fiber filters were ultrasonically extracted three times using sequential solvents of hexane, dichloromethane, and dichloromethane/methanol (9:1, v/v) with activated copper. Then, extracts were derivatized with N,O-bis (trimethylsilyl) trifluoroacetamide (70°C, 60 min). Before gas chromatograph analysis, deuterated n-tetracosane (n-$C_{24}D_{50}$), an internal standard, was used to semi-quantify steroids.

Molecular biomarkers in sediment samples were extracted with organic solvents consistent with that of particles, with the internal standards containing 5α-androstan-3β-ol. The extracts were fractionated into apolar and polar fractions over a silicon column using hexane and methanol as eluents. The polar fraction was saponified with 6% KOH/Methanol at 70°C for 2 h. The acid fraction and the neutral fraction were recovered respectively by hexane (6×). Neutral fractions containing steroids were further

derivatized with N,O-bis (trimethylsilyl) trifluoroacetamide (70°C, 60 min) before analysis.

Steroids in the particulate organic matter were analyzed using an Agilent 7890 A gas chromatography equipped with an Agilent 5977 A mass spectrometer (GC-MS) without internal standard and re-analysed on an Agilent 7890 B gas chromatography equipped with a flame ionized detector (GC-FID) for quantification on cholesterol, with n-tetracosane-d_{50} as an internal standard. The GC-MS and GC-FID both use a DB-5 MS capillary column (60 m × 0.32 mm × 0.25 μm). The GC oven temperature program started at 60°C for 2 min, then increased to 310°C at 3°C min^{-1}, and finally held for 30 min. The MS ion source was operated in electron impact (EI) mode at 230°C with 70 eV electron energy. The MS was operated in full scan mode (m/z 50–750). Concentrations of cholesterol were calculated by comparison of peak area to n-tetracosane-d_{50} on the GC-FID chromatogram. Concentrations of other steroids were conducted by comparison of the area of the characteristic ion of these compounds to that of previously quantified cholesterol.

Steroids of sediments were also analyzed by GC-MS. The GC was equipped with a DB-5 MS capillary column (60 m × 0.32 mm × 0.25 μm). The GC oven temperature program started at 80°C (2 min), then increased to 220°C at 6°C min^{-1}, held for 35 min, to 250°C at 3°C min^{-1}, and finally to 310°C at 2°C min^{-1}. The MS ion source was operated in electron impact (EI) mode at 230 °C with 70 eV electron energy. Full scan was used to identify the biomarkers and single ion monitoring (SIM) for quantitative measurements of C_{27}–C_{29} sterols and stanols. The concentrations of steroids were calculated by comparison of the characteristic ion concentration and the total ion concentration of the internal standard (5α-androstan-3β-ol). For characteristic mass fragments, m/z 215 was used for 5β(H)-cholestan-3β-ol (coprostanol), 5β(H)-cholestan-3α-ol (epicoprostanol), 5α(H)-cholestan-3α-ol (epicholestanol), 5α (H)-cholestan-3β-ol (cholestanol, $C_{27}\Delta^{0}$), 24-methyl-5α (H)-cholestan-3β-ol (campestanol, $C_{28(24Me)}\Delta^{0}$), and 24-ethyl-5α (H)-cholestan-3β-ol (sitostanol, $C_{29(24Et)}\Delta^{0}$); m/z 129 and m/z 255 was used for cholesta-5,22E-dien-3β-ol (22-dehydro-cholesterol, $C_{27}\Delta^{22}$), cholest-5-en-3β-ol (cholesterol, $C_{27}\Delta^{5}$), 24-methylcholesta-5,22-dien-3β-ol (brassicasterol, $C_{28(24Me)}\Delta^{5,22}$), 24-methylcholest-5-en-3β-ol (campesterol, $C_{28(24Me)}\Delta^{5}$), and 24-ethylcholest-5-en-3β-ol (sitosterol, $C_{29(24Et)}\Delta^{5}$) (Nakakuni et al., 2018); m/z 69 and m/z 271 were used for dinosterol (4α,23,24-trimethyl-5α-cholest-22-en-3β-ol).

Analytical uncertainty for the quantification of these biomarkers would be less than 3% based on the repeat analysis of the internal and external standards. All the ratio-based proxies are hardly impacted by the analytical uncertainty and are suitable for the discussion of ratio variations throughout the investigated samples.

2.4 Statistical analyses

Parameters were tested for normality by Shapiro-Wilk-Test. Both two-tailed Pearson correlation coefficients and two-tailed Spearmen correlation coefficients were calculated for the normally and non-normally distributed dataset, respectively. To identify significant differences in POC distribution and biodegradation of SOC across different seasons, one-way ANOVA with Tukey's HSD *post hoc* test was conducted for the normally distributed dataset, while a non-parametric Kruskal–Wallis test for the non-normally distributed dataset. All statistical analyses were considered significant at $p <$

TABLE 1 Environment factors and bulk characteristics of particulate organic carbon (POC) and surface sedimentary organic carbon (SOC) in different layers.

	Layers	May 2018	Sep 2018	Dec 2018	Mar 2019	Jun 2019
Temperature (°C)	Surface	25.6	25.7	12.9	14.0	26.2
	Middle	24.3	25.3	12.8	13.6	25.7
	Bottom	24.1	25.3	12.9	13.1	25.7
DO (mg L^{-1})	Surface	8.87	8.45	7.87	11.27	9.43
	Middle	8.25	7.62	6.36	11.72	8.24
	Bottom	7.80	7.22	8.08	9.72	8.00
POC (mg L^{-1})	Surface	3.20	4.28	2.74	3.80	6.08
	Middle	1.64	3.81	3.12	1.75	6.02
	Bottom	10.11	10.04	2.82	1.88	4.95
$\delta^{13}C_{POC}$ (‰)	Surface	−21.7	−22.2	−25.7	−28.5	−22.8
	Middle	−24.2	−21.9	−25.7	−27.8	−22.6
	Bottom	−23.6	−22.9	−25.6	−27.6	−23.5
TOC (%)	surface sediment	0.78	0.71	0.80	0.85	0.74
$\delta^{13}C_{SOC}$ (‰)	surface sediment	−24.1	−24.1	−24.2	−24.2	−24.2

0.05. All these statistical calculations were performed using the software of SPSS 22.0.

3 Results

3.1 Temperature and DO variations through the investigated annual bloom and decay cycle

During the investigated period, the water temperature at the sampling sites varied from 12.3°C to 27.9°C, with higher water temperatures occurring in the cyanobacterial bloom season (May 2018, September 2018, and June 2019) and lower values in the cyanobacterial decay season (December 2018 and March 2019). The water temperature generally varies synchronously with the *Chlorophyll-A* concentrations and algal densities (Figure 2), per the consensus that water temperature is the main factor influencing the cyanobacterial bloom (optimum temperature above 25°C, Niu et al., 2011; Visser et al., 2016). Along with the cyanobacterial bloom to decay period, the total biomass of phytoplankton decreased in association with the phytoplankton community shifting from the dominance of cyanobacteria (*Microcystis* spp.) to chlorophytes and bacillariophytes (Niu et al., 2011; Guo et al., 2019) or cyanobacteria (*Aphanizomenon* or *Dolichospermum*) (Shan et al., 2019) under low water temperatures. The water temperatures in the vertical water layers were almost the same, indicating no diurnal stratification.

DO values at the sampling sites ranged from 1.5 to 15.1 mg L^{-1}. Monthly average DO values in May 2018, September 2018, December 2018, and June 2019 were 8.3 mg L^{-1}, 7.8 mg L^{-1}, 7.5 mg L^{-1}, and 8.5 mg L^{-1}, respectively (Figure 2; Table 1). Subsequently, DO values rose to 10.9 mg L^{-1} in March. DO values showed no spatial variation in most samples with the same collection date, except for those in December 2018, which showed an obvious increasing trend along the water channel linking Meiliang Bay and the central region. Along the water column, the DO values in the bottom layer are usually 1–2 mg L^{-1} lower than those in the surface layer.

3.2 Organic geochemical characteristics of POC

In Meiliang Bay, POC concentrations ranged from 0.8 to 16.2 mg L^{-1}, with an average value of 4.3 mg L^{-1}. The average POC concentration in the water column increased significantly during the bloom season and dropped rapidly to 1–3 mg L^{-1} during the decay season (ANOVA, $p < 0.05$, Table 1). Additionally, in May 2018 and September 2018, the POC concentrations of water in the bottom layer were higher than those of water in the surface layer (Figure 3A). $\delta^{13}C_{POC}$ values have been widely used to trace the OC of allochthonous (terrestrial plants) and autochthonous sources in lake systems (Raymond and Bauer, 2001; Xu et al., 2020; Wang et al., 2022). The $\delta^{13}C_{POC}$ in Meiliang Bay ranged from −29.5 to −19.9‰, with an average value of −24.4‰. The $\delta^{13}C_{POC}$ showed a significant seasonal difference in POC quality (ANOVA, $p < 0.001$; Figure 3B). The highest monthly average $\delta^{13}C_{POC}$ value was −22.3‰ in September. The lowest monthly average $\delta^{13}C_{POC}$ value was observed in March 2019 (−28.0‰). Meanwhile, the vertical distribution of $\delta^{13}C_{POC}$ values in POC showed different patterns between the bloom and decay seasons, tentatively suggesting different biogeochemical processes (Figure 3B).

Biomarkers for particulate samples also demonstrated the seasonal and vertical dynamics of POC. A series of C_{27}–C_{29} sterols from particulate organic matter was detected in Meiliang Bay (Figures 4A, B). Affected by the relatively high DO content, only traces of stanols were observed throughout the water column, resulting in extremely low $C_{27}\Delta^0/C_{27}\Delta^5$ ratios (near 0). Detailed C_{27}–C_{29} sterol concentrations are listed in Table 2. Among these sterols, cholesterol was the most abundant, followed by sitosterol, brassicasterol, and
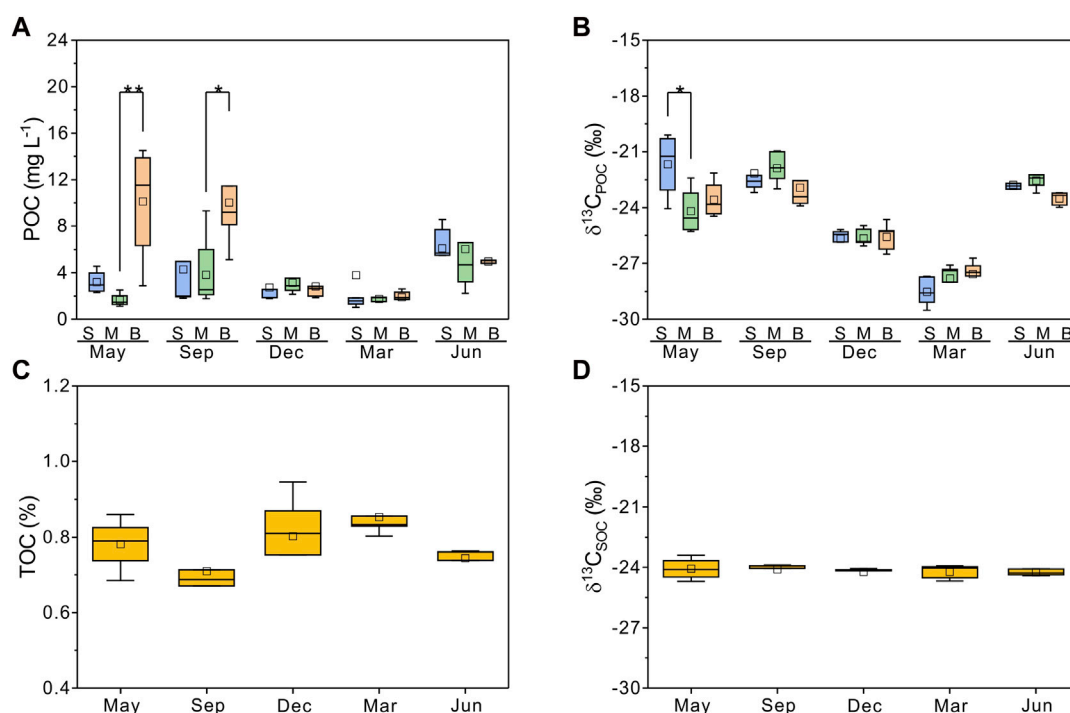
FIGURE 3
Concentrations and stable carbon isotopic compositions of particulate organic carbon (POC, $\delta^{13}C_{POC}$, $n = 77$) and sedimentary organic carbon (TOC, $\delta^{13}C_{SOC}$, $n = 24$). **(A,B)** are POC and $\delta^{13}C_{POC}$ along the water column across seasons, respectively. **(C,D)** are TOC and $\delta^{13}C_{SOC}$ in different seasons. Boxplots show average (hollow point), median (line), first and third quartiles (hinges), and 1IQR (whiskers). The significant difference between POC and $\delta^{13}C_{POC}$ is tested between surface water (S), middle water (M), and bottom water (B). The level of significance from the one-way analysis is reported as *$p < 0.05$ and **$p < 0.01$.
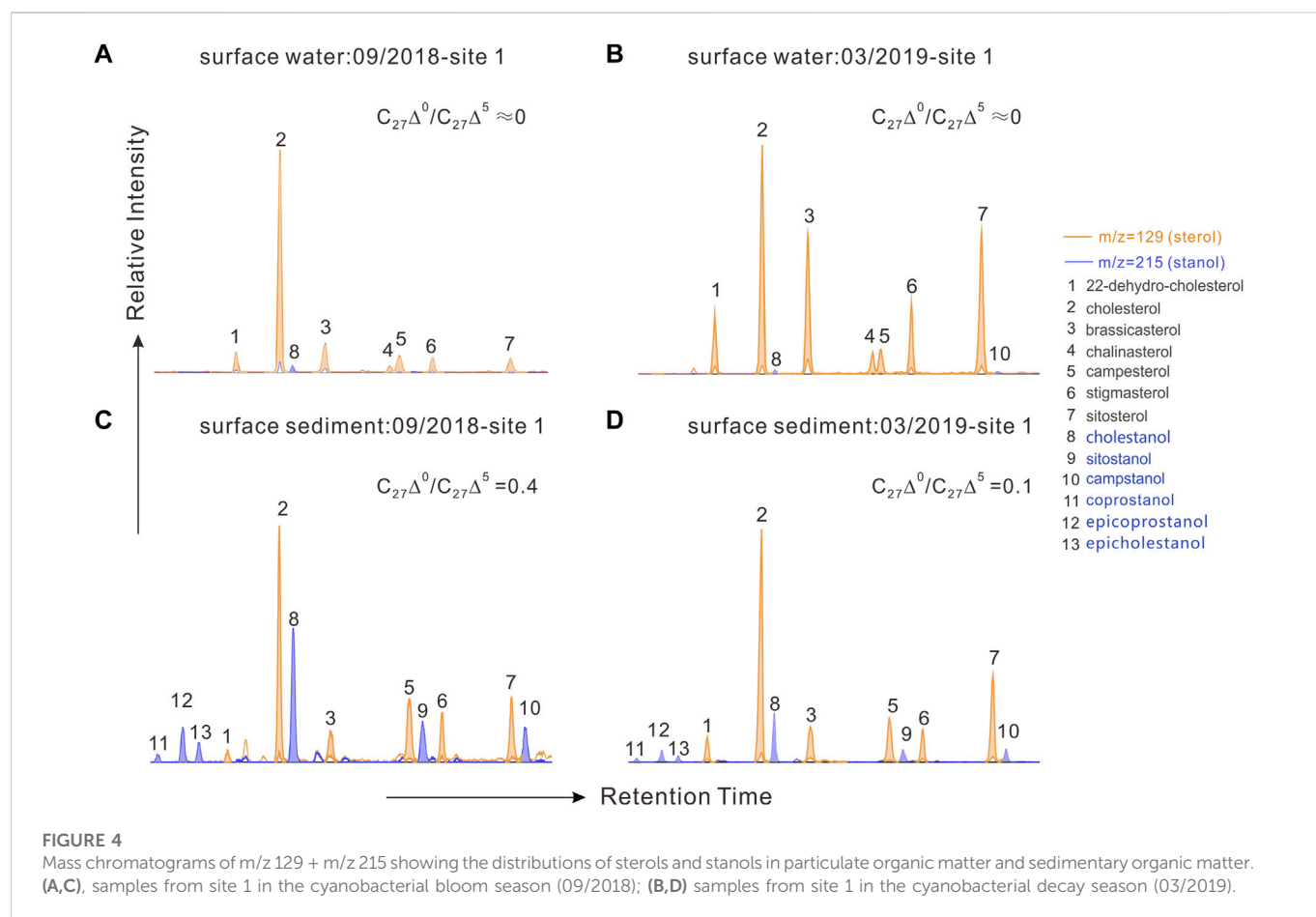
stigmasterol. 22-dehydro-cholesterol, chalinasterol, and campesterol were in low abundance. Dinosterol was detected only in trace amounts in March 2019. The proportion of C_{27} sterols appeared to be significantly higher in the bloom season at 65.7 ± 9.7% than that in the decay season at 44.9 ± 10.4% (ANOVA, $p < 0.001$), while C_{28} and C_{29} sterols increased in the decay season and significantly differed from the bloom season (ANOVA, $p < 0.001$). Along the water depth, the distribution patterns of sterols spanned a much smaller range during the different seasons. For instance, the average proportions of C_{27} sterols showed a decrease from 67.1 ± 10.2% in surface water to 64.4 ± 9.4% in bottom water during the bloom season, accompanied by a very weak increase in C_{28} and C_{29} sterols, implying a preferential decrease in C_{27} sterols during POC sinking (Figure 5D). However, in the decay season, we observed a slight increase in the percentage of C_{27} sterols from 41.6 ± 8.7% to 48.2 ± 11.5%, along with a decrease in C_{28} sterols from 29.2 ± 6.2% to 24.5 ± 7.8% and C_{29} sterols from 29.2 ± 5.6% to 27.2 ± 6.7% (Figure 5D).

3.3 Organic geochemical characteristics of SOC

Compared with POC, sedimentary organic matter was homogeneous. The monthly average TOC content in Meiliang Bay ranged from 0.57% to 0.94%, with an average value of 0.78% (Figure 3C; Table 1). The $\delta^{13}C_{SOC}$ values had a narrow range between −24.7‰ and −23.4‰ with an average value of −24.2‰ (Figure 3D; Table 1).

Although no significant differences in TOC and $\delta^{13}C_{SOC}$ values were observed in samples between the bloom and decay seasons in Meiliang Bay (ANOVA, $p > 0.5$), the relatively higher TOC content in the decay season seems to predict a higher OC sequestration capacity. As for sterols, six regular sterols were detected in the surface sediment, ranked in order of concentration as cholesterol, sitosterol, campesterol, brassicasterol, stigmasterol, and 22-dehydro-cholesterol (Figures 4C, D; Table 2). Chalinasterol was below the detection limit in the surface sediment, but dinosterol was detected at relatively low concentrations ranging from 1.30 to 6.81 µg g^{-1} TOC (Table 2). The total C_{27}–C_{29} sterols concentrations were 80.18–660.93 µg g^{-1} TOC with an average value of 189.38 µg g^{-1} TOC, which was higher than the total concentrations of 5α (H)-stanols and 5β (H)-stanols (83.04–296.83 µg g^{-1} TOC; average 148 µg g^{-1} TOC; Table 2). The anoxic environment of the sediment promoted the transformation of sterols to stanols, resulting in relatively higher $C_{27}\Delta^0/C_{27}\Delta^5$ ratios (0.07–0.51) in comparison to those of POC located in the water column (Table 2). Furthermore, the ratios of $C_{28(24Me)}\Delta^0/C_{28(24Me)}\Delta^5$ and $C_{29(24Et)}\Delta^0/C_{29(24Et)}\Delta^5$ ranged from 0.62 to 1.81, and from 0.27 to 1.44, respectively. Significant seasonal differences in the $C_{27}\Delta^0/C_{27}\Delta^5$, $C_{28(24Me)}\Delta^0/C_{28(24Me)}\Delta^5$, and $C_{29(24Et)}\Delta^0/C_{29(24Et)}\Delta^5$ were observed (ANOVA, $p < 0.001$; Figure 6). All three ratios had their highest values in September 2018 and their lowest values in March 2019.

C_{27} sterols were dominant over the entire period in surface sediment, with an annual average proportion of 51.6 ± 5.3%, together with C_{28} and C_{29} sterols at 23.6 ± 2.9% and 24.8 ± 3.4%,

FIGURE 4
Mass chromatograms of m/z 129 + m/z 215 showing the distributions of sterols and stanols in particulate organic matter and sedimentary organic matter. **(A,C)**, samples from site 1 in the cyanobacterial bloom season (09/2018); **(B,D)** samples from site 1 in the cyanobacterial decay season (03/2019).

respectively. In the bloom season, C_{27} sterols accounted for 49.4 ± 5.3% and the percentages of C_{28} and C_{29} sterols reached 25.5 ± 2.0% and 25.0 ± 4.0%. However, the proportion of C_{28} and C_{29} sterols slightly decreased to 20.9 ± 1.7% and 24.4 ± 2.5%, accompanied by an increase in C_{27} sterols to 54.7 ± 3.8% during the decay season (Figures 5C, D). In addition, higher sterol concentrations were observed during the decay season, especially in March 2019 (Table 2). Therefore, the sediment OC showed a seasonal dynamic due to the different biogeochemical progress in the bloom and decay seasons.

4 Discussion

4.1 Source appointment for steroids in Lake Taihu

Generally, C_{27} sterols in lake environments have been recognized to be mainly produced by eukaryotic phytoplankton or zooplankton (Nishimura and Koyama, 1977; Volkman, 2005; Zhang et al., 2019). In Meiliang Bay, during the investigation period, cholesterol in POC peaked above 61% among C_{27}–C_{29} sterols during the bloom season. POC samples from surrounding rivers are characterized by relatively lower C_{27} sterols and a high proportion of C_{28} and C_{29} sterols (Figures 5A, B; Table 2). Biogeochemical processes within the lake increase the percentage of C_{27} sterols. However, eukaryotic

phytoplankton including diatoms, dinoflagellates, and green algae have a limited distribution in the cyanobacterial bloom season (Niu et al., 2011; Su et al., 2017; Guo et al., 2019), implying the trace C_{27} sterols input. As for the zooplankton, it grows in tandem with cyanobacteria in Lake Taihu for highly effective consumption of cyanobacteria-derived carbon via bacteria pathways and direct grazing (de Kluijver et al., 2012). Therefore, zooplankton is an important source of C_{27} sterols. However, the concentration of C_{27} sterols is surprisingly quite low in September 2019, opposite to the trend of zooplankton biomass. This phenomenon suggests that there are other important origins of C_{27} sterols besides eukaryotes, such as cyanobacteria. Volkman (2005) suggested that some specific cyanobacterial species, including *Microcystis* dominant in Lake Taihu, could synthesize small amounts of sterols (typically below 0.03% of the cell dry weight) in the organism. In Meiliang Bay, biomarkers of cyanobacterial extracts also suggested that cyanobacteria mainly produce cholesterol (60.1%) and minor sitosterol (32.1%) (Figures 5A, B). Therefore, we suggest that the relatively high proportion of C_{27} sterols is most likely caused by a large number of cyanobacteria in Meiliang Bay, in addition to the common eukaryotic contribution.

C_{28} sterols, including brassicasterol and chalinasterol, have been recognized as indicators of diatom sources (Volkman, 2005; Köseoğlu et al., 2019). Over the investigated period, brassicasterol showed a weak positive correlation with C_{27}

TABLE 2 Biomarker concentrations and parameters for surface and bottom water particulate organic matter and surface sedimentary organic matter in different months.

	May 2018	Sep 2018	Dec 2018	Mar 2019	Jun 2019
Surface water					
22-dehydro-cholesterol ($\mu g\ L^{-1}$)	0.03	0.05	0.05	0.52	0.20
Cholesterol ($\mu g\ L^{-1}$)	0.67	0.89	0.29	1.66	2.68
Brassicasterol ($\mu g\ L^{-1}$)	0.19	0.06	0.13	1.47	0.49
Chalinasterol ($\mu g\ L^{-1}$)	0.03	0.01	0.03	0.34	0.05
Campesterol ($\mu g\ L^{-1}$)	0.10	0.09	0.03	0.31	0.22
Stigmasterol ($\mu g\ L^{-1}$)	0.06	0.04	0.03	0.45	0.18
Sitosterol ($\mu g\ L^{-1}$)	0.09	0.08	0.17	1.67	0.32
C_{27} sterol (%)[a]	57.8	73.0	48.6	34.6	68.7
C_{28} sterol (%)[b]	28.0	16.4	24.8	33.6	21.4
C_{29} sterol (%)[c]	14.2	10.6	26.5	31.8	9.9
Bottom water					
22-dehydro-cholesterol ($\mu g\ L^{-1}$)	0.09	0.04	0.10	0.79	0.21
Cholesterol ($\mu g\ L^{-1}$)	1.45	0.58	0.51	2.74	2.71
Brassicasterol ($\mu g\ L^{-1}$)	0.30	0.06	0.14	1.86	0.38
Chalinasterol ($\mu g\ L^{-1}$)	0.16	0.01	0.03	0.32	0.01
Campesterol ($\mu g\ L^{-1}$)	0.22	0.08	0.05	0.45	0.29
Stigmasterol ($\mu g\ L^{-1}$)	0.16	0.06	0.04	0.50	0.23
Sitosterol ($\mu g\ L^{-1}$)	0.33	0.07	0.27	1.96	0.34
C_{27} sterol (%)[a]	57.8	66.0	54.9	41.6	67.9
C_{28} sterol (%)[b]	24.3	18.1	19.4	29.6	18.9
C_{29} sterol (%)[c]	17.9	15.9	25.7	28.8	13.2
Surface sediment					
22-dehydro-cholesterol ($\mu g\ g^{-1}$ TOC)	7.23	3.54	5.44	15.26	7.44
Cholesterol ($\mu g\ g^{-1}$ TOC)	81.24	48.98	71.31	152.73	92.43
Brassicasterol ($\mu g\ g^{-1}$ TOC)	24.49	11.10	11.22	33.48	20.36
Campesterol ($\mu g\ g^{-1}$ TOC)	25.04	18.24	16.80	33.81	26.15
Stigmasterol ($\mu g\ g^{-1}$ TOC)	16.70	11.97	10.43	24.12	14.37
Sitosterol ($\mu g\ g^{-1}$ TOC)	34.01	18.86	21.09	61.37	27.55
Dinosterol ($\mu g\ g^{-1}$ TOC)	3.77	3.87	2.39	3.69	3.32
Coprostanol ($\mu g\ g^{-1}$ TOC)	4.90	4.40	4.03	6.48	6.75
Epicoprostanol ($\mu g\ g^{-1}$ TOC)	15.35	18.58	15.72	17.69	22.75
Epicholestanol ($\mu g\ g^{-1}$ TOC)	6.47	10.36	7.66	11.23	11.14
Cholestanol ($\mu g\ g^{-1}$ TOC)	59.38	74.61	55.18	80.23	75.28
Campestanol ($\mu g\ g^{-1}$ TOC)	22.13	26.97	19.59	25.63	28.16
Sitostanol ($\mu g\ g^{-1}$ TOC)	21.14	23.18	15.96	23.11	22.92
$C_{27}\Delta^{0}/C_{27}\Delta^{5}$	0.2	0.4	0.2	0.1	0.2
$C_{28(24Me)}\Delta^{0}/C_{28(24Me)}\Delta^{5}$	1.0	1.5	1.2	0.9	1.1
$C_{29(24Et)}\Delta^{0}/C_{29(24Et)}\Delta^{5}$	0.7	1.3	0.8	0.5	0.9
C_{27} sterol (%)[a]	48.2	46.0	55.6	53.7	53.9
C_{28} sterol (%)[b]	25.7	26.5	20.8	21.0	24.4
C_{29} sterol (%)[c]	26.1	27.5	23.5	25.3	21.7

[a]C_{27} sterol (%) = (22-dehydro-cholesterol + cholesterol)/(22-dehydro-cholesterol + cholesterol + brassicasterol + chalinasterol + campesterol + stigmasterol + sitosterol).

[b]C_{28} sterol (%) = (brassicasterol + chalinasterol + campesterol)/(22-dehydro-cholesterol + cholesterol + brassicasterol + chalinasterol + campesterol + stigmasterol + sitosterol).

[c]C_{29} sterol (%) = (stigmasterol + sitosterol)/(22-dehydro-cholesterol + cholesterol + brassicasterol + chalinasterol + campesterol + stigmasterol + sitosterol).

sterols ($r^2 = 0.48$, $p < 0.001$, $n = 48$), tentatively suggesting that the bioproduction of the diatom did not keep pace with the cyanobacteria. Campesterol can also be regarded as a biomarker for diatom, considering its higher Pearson correlation coefficients with brassicasterol and chalinasterol ($r^2 = 0.7$, $r^2 = 0.6$, $p < 0.001$, $n = 48$). Therefore, although C_{28} sterols might not be as sensitive as C_{27} sterols, they should also be considered when tracking the relative contribution of OC from different kinds of phytoplankton.

Among the C_{29} sterols, sitosterol is usually the main sterol in vascular plants (Meyers, 1997; Volkman et al., 1998). Although a

phytoplankton source cannot be excluded (Zhang et al., 2017a), stigmasterol was also interpreted as a terrestrial OC source, considering its good match with sitosterol ($r^2 = 0.8$, $p < 0.001$, $n = 48$). Dinosterol is a highly specific biomarker for dinoflagellates (Robinson et al., 1984). However, considering the trace amount of dinosterol in the POC pool, dinoflagellates might only make a small contribution to *in-situ* bioproduction. In this sense, the distribution pattern of sterols could sensitively respond to changes in OC sources in SOC and POC, with C_{27} and C_{29} signaling cyanobacterial and terrestrial OC, respectively.
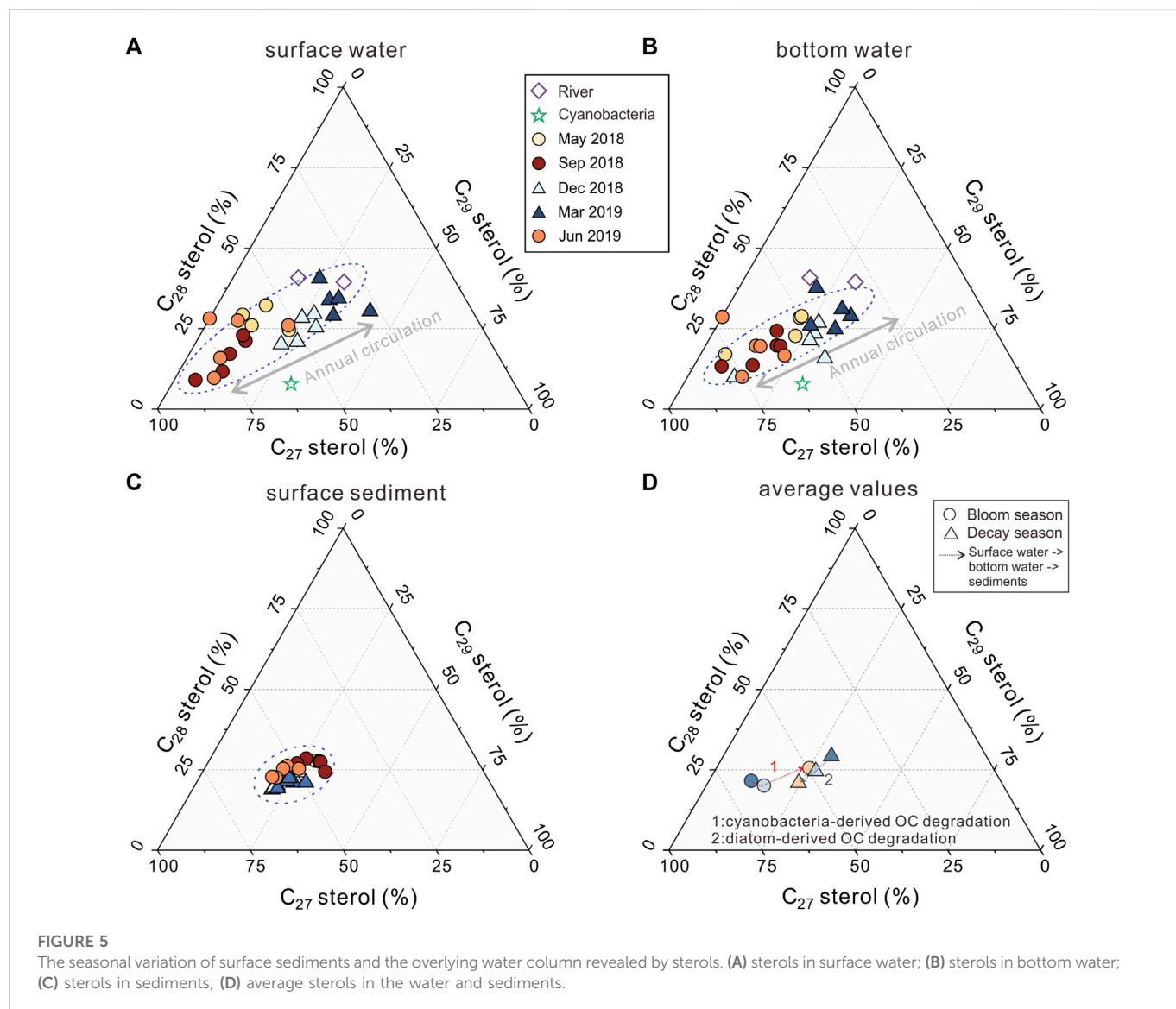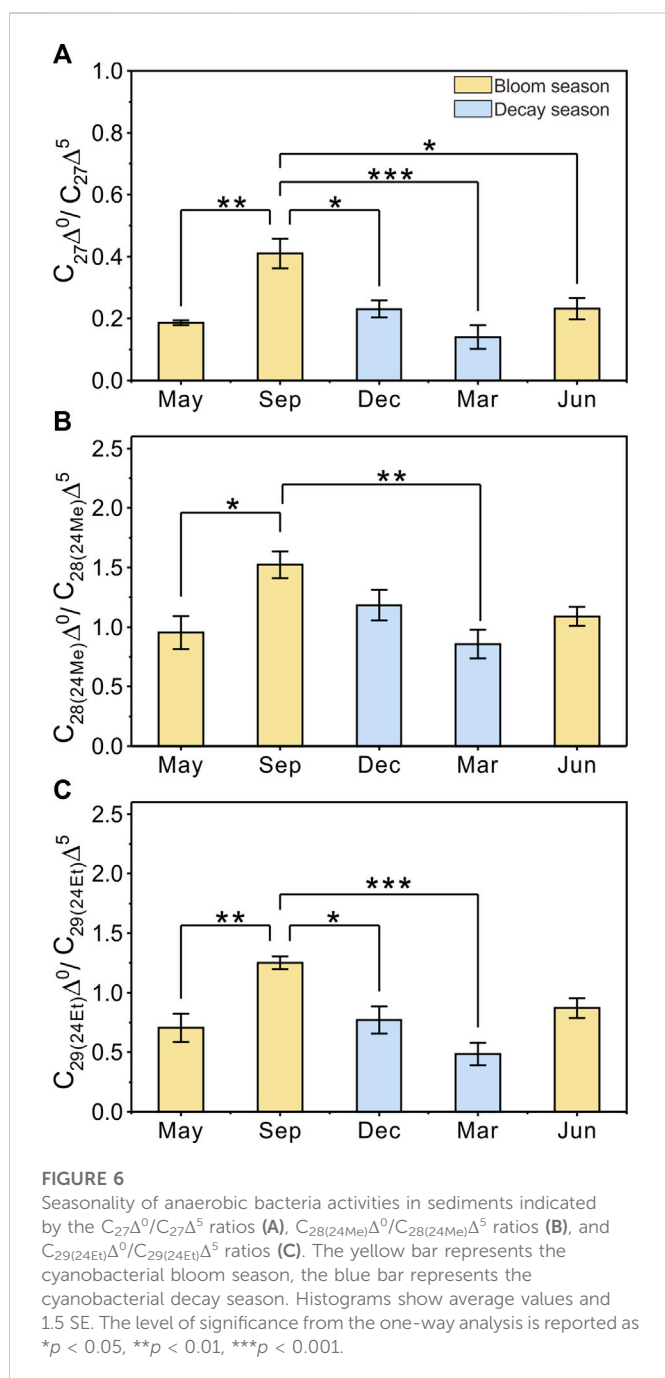
FIGURE 5
The seasonal variation of surface sediments and the overlying water column revealed by sterols. **(A)** sterols in surface water; **(B)** sterols in bottom water; **(C)** sterols in sediments; **(D)** average sterols in the water and sediments.

4.2 Seasonal variations in the sources of POC and SOC

4.2.1 Strong seasonal variations in POC

The seasonal bloom and succession of phytoplankton in Meiliang Bay shape the POC pool, as evidenced by $\delta^{13}C_{POC}$ and biomarkers. In Meiliang Bay, the higher $\delta^{13}C_{POC}$ in the bloom season approached the cyanobacterial signal at −20.5‰ (Xu et al., 2020; Meng et al., 2021), suggesting the dominant cyanobacteria-derived OC input. A similar trend of $\delta^{13}C_{POC}$ with *Chlorophyll-A* concentrations and phytoplankton densities indicates that the cyanobacterial bloom event is the determining factor in the POC pool, whereas $\delta^{13}C_{POC}$ along the water column spanning approximately 1‰–2‰ implies less influence of sinking progress and sediment resuspension, both of which occur frequently in shallow lakes (Tang et al., 2020; Wang et al., 2022). Simultaneously, a significantly higher proportion of C_{27} sterols among the C_{27}–C_{29} sterols than riverine samples also suggests the increasing zooplankton and an additional supply of cyanobacteria-derived OC within the lake, further supporting the notion that cyanobacteria contribute a large amount of labile OC to

the total POC pool in Meiliang bay (Xu et al., 2019; Meng et al., 2021). However, during the decay season, terrestrial OC became the major source of POC in Meiliang Bay. In March, the lowest average $\delta^{13}C_{POC}$ value (−28.0‰) suggests a strong contribution from allochthonous OC derived from river transportation and soil erosion in the Taihu Basin (Xu et al., 2020). Additionally, sitosterol and stigmasterol were present in high proportions during the decay season (Figures 5A, B; Table 2). Along with the rapid decrease in cyanobacterial biomass, the enhanced bio-productivity of Bacillariophyta, Chlorophyta, Chrysophyta, and Cryptophyta in winter (Su et al., 2017) would contribute to POC, as shown by the higher proportion of C_{28} sterols. Therefore, terrestrial OC and eukaryotic phytoplankton peaked during the cyanobacterial decay season, as revealed by the enhanced C_{28}–C_{29} sterols, differing from the cyanobacterial bloom season. Considering that the average POC concentration in the water column increased significantly during the bloom season (ANOVA, $p < 0.05$, Table 1), seasonal variation in POC is largely controlled by the phytoplankton bio-productivity accumulated at the water surface in the bloom season.

FIGURE 6
Seasonality of anaerobic bacteria activities in sediments indicated by the $C_{27}\Delta^0/C_{27}\Delta^5$ ratios **(A)**, $C_{28(24Me)}\Delta^0/C_{28(24Me)}\Delta^5$ ratios **(B)**, and $C_{29(24Et)}\Delta^0/C_{29(24Et)}\Delta^5$ ratios **(C)**. The yellow bar represents the cyanobacterial bloom season, the blue bar represents the cyanobacterial decay season. Histograms show average values and 1.5 SE. The level of significance from the one-way analysis is reported as *$p < 0.05$, **$p < 0.01$, ***$p < 0.001$.

4.2.2 Relatively weak seasonal variations in SOC

In sediments, SOC shows a weak seasonal pattern, as revealed by sterols, although SOC is relatively consistent compared to POC. In the bloom season, $\delta^{13}C_{SOC}$ values (average of $-24.1‰$) implied a mixture of terrestrial and cyanobacteria-derived OC. However, the relatively lower C_{27} sterol proportion in the bloom season compared to the decay season implies that SOC is characterized by a slightly lower input from cyanobacteria-derived OC during the bloom season (Figures 5C, D). At the same time, the lower TOC content of sediment samples collected during the bloom season also showed no accumulation of SOC from massive primary productivity (Table 1). In the decay season, comparable or slightly higher amounts of cyanobacteria-derived OC were buried in the sediment, as

indicated by a slightly higher proportion of C_{27} sterols (decay vs. bloom, 54.6% vs. 49.4%) and higher TOC (decay vs. bloom, 0.82% vs. 0.74%). Although seasonal variations in SOC were still observed at the molecular level (i.e., sterol), the variation in the sterol distribution of SOC was still very weak, which can be alternatively interpreted by the uncertainties of these diagnostic proxies. In contrast, $\delta^{13}C_{SOC}$ remained unchanged throughout the investigated period (decay vs. bloom, $-24.1‰$ vs. $-24.2‰$). It is possible that $\delta^{13}C_{SOC}$ is representative of the bulk characteristics of SOC, including terrestrial OC, cyanobacteria-derived OC, and heterotrophic bacteria-derived OC in eutrophic lakes (Lu and Meyers, 2009; Naeher et al., 2012; Xu et al., 2015a; 2015b; Zhang et al., 2017a); therefore, it is not very sensitive to very small seasonal variations in SOC. As a result, we believe that the source of SOC remains roughly stable, even during very strong seasonal blooms and the successions of phytoplankton.

4.3 Contrasting OC burial behaviors between bloom and decay seasons

The changes in the distribution pattern of sterols in POC and SOC between bloom and decay seasons demonstrate contrasting seasonal behaviors during OC settlement and burial at the water column and water-sediment interfaces. For instance, during the decay season, when POC is dominated by refractory terrestrial sources, the sterol distribution patterns are similar in surface water, bottom water, and surface sediments. At the water column and water-sediment interface, we observed a slight increase in the percentage of C_{27} sterols, accompanied by the decrease of C_{28} and C_{29} sterols (Figure 5D). Therefore, the degradation behavior of cyanobacteria-derived OC is not the main controlling factor for OC burial during the decay season, considering that SOC is more labile and cyanobacteria-derived than POC above the sediments. We suspect that the slight increase in the percentages of C_{27} sterols in sediments might be due to the degradation of diatom-derived OC, which is the main source of C_{28} sterols. Alternatively, SOC is a mixture of cyanobacteria-derived and allochthonous OC, whereas POC is primarily allochthonous OC dominated by C_{28} and C_{29} sterols. Nevertheless, further investigations are required in the future.

During the bloom season, from surface water to bottom water, the sterol distribution patterns were roughly similar, with only an approximately 2.7% decrease in the proportion of C_{27} sterols (Figure 5D). These results indicate that, although cyanobacteria-derived carbon is utilized in the water medium, such a degradation effect is not intensive enough to show significant changes in the OC characteristics through the water column. However, from bottom water to surface sediment, we found that the OC strongly shifted to a terrestrial OC source. For instance, C_{27} sterols only account for 49.4% of the surface sediments, which is approximately 15% less than those in bottom water (Figure 5D). Such changes can also be seen in the more negative $\delta^{13}C$ values of SOC than POC at the bottom layer (Table 1). Together, these results indicate a relatively lower accumulation of cyanobacteria-derived OC in the sediment when sinking OC from the upper layer was high during the bloom season.

In Meiliang bay, the maximum POC concentration occurs during the summer season, largely due to massive cyanobacteria-derived OC input from cyanobacterial blooms (Jiang et al., 2015; Huang et al., 2019). From the similar distribution of sterols in the water column,

bioproduction is more important than the effect of degradation at this exact place. Thus, during the particulate settling process through the water column, the balance between the OC sinking flux and initial OC input does not change systematically with the increased proportion of labile OC. At the water-sediment interface on the other hand, further degradation of cyanobacteria-derived OC proceeds in the interface by heterotrophic bacteria (Meyers and Ishiwatari, 1993; Liu et al., 2022), as indicated by the rapid decrease of C_{27} sterol proportion (Figure 5D). Compared with the decay season, the proportion of C_{27} sterols from sediments in the bloom season is even less, suggesting that extensive degradation of OC in the water-sediment interface in the bloom season could even reverse the seasonal distribution characteristics of particulate OC in the water column, and eventually lead to less accumulation of OC (as inferred by lower TOC values, Table 1) under the background of higher cyanobacteria-derived OC input. In this sense, cyanobacteria-derived OC in the bloom season is poorly preserved in the sediments. Over the past decade, although the sedimentary TOC values in Meiliang Bay have slightly increased from its natural background of 0.6% (before the 1980 s) to approximately 1% (Gui et al., 2013), they are still lower than that in other Chinese subtropical eutrophic lakes, such as Lake Donghu (~3.5%), Lake Erhai (~10%), and Lake Honghu (~8%) (Yang et al., 2008; Zhang et al., 2017b). Also, OC burial flux in the studied region of Lake Taihu is lower than that of Lake Okeechobee with a similar eutrophication level (28 vs. 60 g C m^{-2} yr^{-1}, Dong et al., 2012; Gui et al., 2013). These pieces of evidence further support the notion that eutrophication has not been effective in enhancing long-term carbon burial in Lake Taihu.

Indeed, similar phenomena can be also found in eutrophic Lake Hachiro, where sedimentary TOC accumulates with terrestrial and diatom-derived OC in winter and spring, despite the delivery peak of cyanobacteria-derived OC in summer (Fujibayashi et al., 2019). The seasonal variation in POC and SOC clearly shows that the accumulation of cyanobacteria-derived carbon occurs in winter with low primary productivity, resulting in low OC burial efficiency throughout the year. Accordingly, case studies in Lake Taihu and Lake Hachiro confirm that the accumulation of cyanobacteria-derived OC is difficult in shallow subtropical lakes. The stronger degradation characteristics of cyanobacteria-derived OC might be related to the quality of cyanobacteria-derived OC, considering it has a much quicker turnover time (60%–80% of OC can be decomposed in days or weeks, Hanamachi et al., 2008; Li et al., 2012; Bai et al., 2017). Besides, cyanobacteria-derived OC can shape bacterial communities for more effective degradation (Berry et al., 2017; Zhu et al., 2019). However, the OC quality alone could hardly be the sole reason for the lower OC burial under the overwhelming labile cyanobacteria-derived OC input at the first step, asking for additional controlling factors to be included in the framework.

4.4 Contributors for stronger OC loss in shallow subtropical lakes

As discussed above, the strong cyanobacterial input under severe eutrophication could be limited to modifying the SOC in shallow subtropical lakes like Lake Taihu, largely owing to the rapid loss of OC during the particulate settling process. Multiple factors other than the amount and source of the OC could affect OC mineralization rates with seasonal variation, such as temperature (Gudasz et al., 2010; Cardoso et al.,

2014), oxygen exposure (Sobek et al., 2009; Wang et al., 2018), and the potential consumption of OC by microorganisms (Tabuchi et al., 2010; Cai et al., 2014). Firstly, temperature, as a determining factor in modulating biological processes, might be strongly attributed to seasonal OC degradation rates. In summer and autumn, high temperatures in the water column would also facilitate the metabolism of organisms, leading to higher OC mineralization rates and, consequently, less carbon burial (Gudasz et al., 2010; Cardoso et al., 2014). The biomass of heterotrophic bacteria peaked during the hot summer months in water and sediments (Canuel and Martens, 1993; Niu et al., 2011), further promoting OC degradation. According to the prediction models of temperature and metabolic processes in sediments, OC mineralization rates decreased 2-3 times when the temperature dropped by 10°C in temperate aquatic ecosystems (Gudasz et al., 2010). Therefore, the degradation rate of OC at the water-sediment interface could be high in the summer and decrease further in the winter. However, in Meiliang Bay, the increasing temperature in Lake Taihu prolongs cyanobacterial growth and extends the bloom season (Salk et al., 2022), which is counteracted by temperature-dependent respiratory losses due to increased microbial and enzymatic activity (Tabuchi et al., 2010; Patel et al., 2019). Based on the results of this study, we suggest that the fast degradation rate of labile OC in shallow lakes bypasses the accumulation rate of cyanobacteria-derived OC during the bloom season. This is consistent with a recent study that found Lake Taihu to be a CO_2 source over the last 24 years (1992–2015) despite global warming (Xiao et al., 2022).

Secondly, strong oxygen exposure might be largely linked to impeded OC preservation (Sobek et al., 2009; Wang et al., 2018; Wei et al., 2022). In the bloom season, the high cyanobacteria-derived OC mineralization rates would lead to a relatively anaerobic environment by consuming oxygen through the water column (Cai et al., 2014; Yan et al., 2019). However, oxygen accumulated from the photosynthesis of phytoplankton on the lake surface could compensate for the oxygen consumption by cyanobacteria-derived OC mineralization and prevent the water from hypoxia condition (DO < 2 mg L^{-1}). Also, strong water mixing disturbed by wind in summer seasons maintains an oxidizing environment (Jalil et al., 2018) suitable for continuous OC mineralization in shallow aquatic ecosystems (Wang et al., 2018; Wei et al., 2022). Therefore, high oxygen exposure and the sustained oxidizing environment during the whole year guarantee the highly effective OC loss through the water column in shallow subtropical lakes. Interestingly, the DO values in the bottom layer are usually 1-2 mg L^{-1} lower than those in the surface layer (Table 1), tentatively suggesting that the effect of oxygen exposure mainly occurred on the upper section of the water column. In this sense, oxygen exposure might not be an important contributor to the OC loss at the water-sediment interface.

Thirdly, active anaerobic microorganism activities in sediment should be considered for the strong OC mineralization in eutrophic lakes (Bechtel and Schubert, 2009; Yan et al., 2019). The redox potential in sediments can greatly decrease within 0–3 cm after the decomposition of sinking OC during the bloom season in Lake Taihu (Zhao et al., 2007), further promoting anaerobic degradation such as methanogens processes (Yan et al., 2019). The highest ratios of $C_{27}\Delta^0/C_{27}\Delta^5$, $C_{28(24Me)}\Delta^0/C_{28(24Me)}\Delta^5$, and $C_{29(24Et)}\Delta^0/C_{29(24Et)}\Delta^5$ observed in September 2018 indicate a strong anaerobic microbial modification of SOC, and the lowest ratios in March reveal the silence of microbial activities (Figure 6). These seasonal bacterially-mediated processes in eutrophic lakes is an inescapable contributor to OC degradation. Considering that OC degradation

becomes much stronger at the water-sediment interface, anaerobic microorganisms situated in the surface sediment might be a more important contributor in the case of Lake Taihu.

In summary, the combined effect of factors including OC bioavailability, temperature, oxygen exposure, and more importantly microorganism activities, eventually results in much higher OC degradation rates, canceling out the potential OC sink effect from lake eutrophication. Considering that eutrophication destroys the ecosystem of lakes and their catchments, it is an urgent issue to be solved with extensive efforts in the future.

5 Conclusion

(1) In hypereutrophic Meiliang Bay, cyanobacterial blooms bring a considerable amount of cyanobacteria-derived POC to the water column, as revealed by the heavy $\delta^{13}C_{POC}$ and predominance of C_{27} sterols. In contrast, terrestrial OC was the main contributor to POC in the cyanobacterial decay season, accompanied by an increase in eukaryotic phytoplankton such as diatoms. SOC showed a weak seasonal dynamic, characterized by slightly lower cyanobacteria-derived OC in the bloom season than in the decay season.

(2) Given the similar distributions of C_{27}–C_{29} sterols in surface and bottom water, the delivery of POC into the bottom water layer still mainly inherits lake productivity in the surface water column. However, extensive degradation of SOC in the bloom season reverses the seasonal distribution characteristics of POC, leading to less accumulation of OC under the background of higher cyanobacteria-derived OC input from the overlying water.

(3) In subtropical shallow lakes like Lake Taihu, the OC bioavailability, temperature, oxygen exposure, and more importantly microorganism activities, significantly increase OC mineralization rates in the bloom season. The resulting asymmetric deposition pattern between POC and SOC suggests that eutrophication has less influence on OC burial when compared to other factors related to OC degradation.

Data availability statement

The raw data supporting the conclusions of this article will be made available by the authors, without undue reservation.

Author contributions

YX, YH, and YS contributed to the conception and design of the study. YX and JP contributed to fieldwork and lab experiments. YX and YH analyzed the data and wrote the draft of the manuscript. All authors have contributed to the revision and improvement of the manuscript.

Conflict of interest

The authors declare that the research was conducted in the absence of any commercial or financial relationships that could be construed as a potential conflict of interest.

Publisher's note

All claims expressed in this article are solely those of the authors and do not necessarily represent those of their affiliated organizations, or those of the publisher, the editors and the reviewers. Any product that may be evaluated in this article, or claim that may be made by its manufacturer, is not guaranteed or endorsed by the publisher.

References

Anderson, N. J., Bennion, H., and Lotter, A. F. (2014). Lake eutrophication and its implications for organic carbon sequestration in Europe. *Glob. Change Biol.* 20 (9), 2741–2751. doi:10.1111/gcb.12584

Bai, L., Cao, C., Wang, C., Xu, H., Zhang, H., Slaveykova, V. I., et al. (2017). Toward quantitative understanding of the bioavailability of dissolved organic matter in freshwater lake during cyanobacteria blooming. *Environ. Sci. Technol.* 51 (11), 6018–6026. doi:10.1021/acs.est.7b00826

Bechtel, A., and Schubert, C. J. (2009). A biogeochemical study of sediments from the eutrophic Lake Lugano and the oligotrophic Lake Brienz, Switzerland. *Org. Geochem.* 40 (10), 1100–1114. doi:10.1016/j.orggeochem.2009.06.009

Berry, M. A., Davis, T. W., Cory, R. M., Duhaime, M. B., Johengen, T. H., Kling, G. W., et al. (2017). Cyanobacterial harmful algal blooms are a biological disturbance to Western Lake Erie bacterial communities. *Environ. Microbiol.* 19 (3), 1149–1162. doi:10.1111/1462-2920.13640

Cai, H., Jiang, H., Krumholz, L. R., and Yang, Z. (2014). Bacterial community composition of size-fractioned aggregates within the phycosphere of cyanobacterial blooms in a eutrophic freshwater lake. *PLoS One* 9 (8), e102879. doi:10.1371/journal.pone.0102879

Canuel, E. A., and Martens, C. S. (1993). Seasonal variations in the sources and alteration of organic matter associated with recently-deposited sediments. *Org. Geochem.* 20 (5), 563–577. doi:10.1016/0146-6380(93)90024-6

Cardoso, S. J., Enrich-Prast, A., Pace, M. L., and Rol, F. (2014). Do models of organic carbon mineralization extrapolate to warmer tropical sediments? *Limnol. Oceanogr.* 59 (1), 48–54. doi:10.4319/lo.2014.59.1.0048

de Kluijver, A., Yu, J., Houtekamer, M., Middelburg, J. J., and Liu, Z. (2012). Cyanobacteria as a carbon source for zooplankton in eutrophic Lake Taihu, China, measured by ^{13}C labeling and fatty acid biomarkers. *Limnol. Oceanogr.* 57 (4), 1245–1254. doi:10.4319/lo.2012.57.4.1245

Dong, X., Anderson, N. J., Yang, X., Chen, X., and Shen, J. (2012). Carbon burial by shallow lakes on the Yangtze floodplain and its relevance to regional carbon sequestration. *Glob. Change Biol.* 18 (7), 2205–2217. doi:10.1111/j.1365-2486.2012.02697.x

Fujibayashi, M., Ashino, M., Okano, K., and Miyata, N. (2019). Spatial and seasonal variability of sedimentary organic matter and its origin in an algal-blooming eutrophic lake. *Ecol. Indic.* 107, 105557. doi:10.1016/j.ecolind.2019.105557

Gudasz, C., Bastviken, D., Steger, K., Premke, K., Sobek, S., and Tranvik, L. J. (2010). Temperature-controlled organic carbon mineralization in lake sediments. *Nature* 466 (7305), 478–481. doi:10.1038/nature09186

Gui, Z., Xue, B., Yao, S., Wei, W., and Yi, S. (2013). Organic carbon burial in lake sediments in the middle and lower reaches of the Yangtze River Basin, China. *Hydrobiologia* 710 (1), 143–156. doi:10.1007/s10750-012-1365-9

Guillemette, F., von Wachenfeldt, E., Kothawala, D. N., Bastviken, D., and Tranvik, L. J. (2017). Preferential sequestration of terrestrial organic matter in boreal lake sediments. *J. Geophys. Res. Biogeosciences* 122 (4), 863–874. doi:10.1002/2016JG003735

Guo, C., Zhu, G., Qin, B., Zhang, Y., Zhu, M., Xu, H., et al. (2019). Climate exerts a greater modulating effect on the phytoplankton community after 2007 in eutrophic Lake Taihu, China: Evidence from 25 years of recordings. *Ecol. Indic.* 105, 82–91. doi:10.1016/j.ecolind.2019.05.034

Hanamachi, Y., Hama, T., and Yanai, T. (2008). Decomposition process of organic matter derived from freshwater phytoplankton. *Limnology* 9 (1), 57–69. doi:10.1007/s10201-007-0232-2

He, W., Chen, M., Schlautman, M. A., and Hur, J. (2016). Dynamic exchanges between dom and pom pools in coastal and inland aquatic ecosystems: A review. *Sci. Total Environ.* 551–552, 415–428. doi:10.1016/j.scitotenv.2016.02.031

Huang, C., Zhang, Y., Huang, T., Yang, H., Li, Y., Zhang, Z., et al. (2019). Long-term variation of phytoplankton biomass and physiology in Taihu lake as observed via MODIS satellite. *Water Res.* 153, 187–199. doi:10.1016/j.watres.2019.01.017

Huisman, J., Codd, G. A., Paerl, H. W., Ibelings, B. W., Verspagen, J. M. H., and Visser, P. M. (2018). Cyanobacterial blooms. *Nat. Rev. Microbiol.* 16 (8), 471–483. doi:10.1038/s41579-018-0040-1

Jalil, A., Li, Y., Du, W., Wang, W., Wang, J., Gao, X., et al. (2018). The role of wind field induced flow velocities in destratification and hypoxia reduction at Meiling Bay of large shallow Lake Taihu, China. *Environ. Pollut.* 232, 591–602. doi:10.1016/j.envpol.2017.09.095

Jiang, G., Ma, R., Loiselle, A. S., Duan, H., Su, W., Cai, W., et al. (2015). Remote sensing of particulate organic carbon dynamics in a eutrophic lake (Taihu Lake, China). *Sci. Total Environ.* 532, 245–254. doi:10.1016/j.scitotenv.2015.05.120

Kiersztyn, B., Chróst, R., Kaliński, T., Siuda, W., Bukowska, A., Kowalczyk, G., et al. (2019). Structural and functional microbial diversity along a eutrophication gradient of interconnected lakes undergoing anthropopressure. *Sci. Rep.* 9 (1), 11144. doi:10.1038/s41598-019-47577-8

Köseoğlu, D., Belt, S. T., and Knies, J. (2019). Abrupt shifts of productivity and sea ice regimes at the Western Barents Sea slope from the Last Glacial Maximum to the Bølling-Allerød interstadial. *Quat. Sci. Rev.* 222, 105903. doi:10.1016/j.quascirev.2019.105903

Kosten, S., Huszar, V. L. M., Bécares, E., Costa, L. S., van Donk, E., Hansson, L. A., et al. (2012). Warmer climates boost cyanobacterial dominance in shallow lakes. *Glob. Change Biol.* 18 (1), 118–126. doi:10.1111/j.1365-2486.2011.02488.x

Li, H., and Minor, E. C. (2015). Biogeochemical characteristics of settling particulate organic matter in Lake superior: A seasonal comparison. *Org. Geochem.* 85, 76–88. doi:10.1016/j.orggeochem.2015.05.006

Li, L., Gao, N., Deng, Y., Yao, J., and Zhang, K. (2012). Characterization of intracellular & extracellular algae organic matters (AOM) of Microcystic aeruginosa and formation of AOM-associated disinfection byproducts and odor & taste compounds. *Water Res.* 46 (4), 1233–1240. doi:10.1016/j.watres.2011.12.026

Li, Z., Li, X., Wang, X., Ma, J., Xu, J., Xu, X., et al. (2020). Isotopic evidence revealing spatial heterogeneity for source and composition of sedimentary organic matters in Taihu Lake, China. *Ecol. Indic.* 109, 105854. doi:10.1016/j.ecolind.2019.105854

Liu, X., Wendt, K., Barth, J. A. C., and Friese, K. (2022). Post-depositional alteration of stable isotope signals by preferential degradation of algae-derived organic matter in reservoir sediments. *Biogeochemistry* 159, 315–336. doi:10.1007/s10533-022-00930-y

Lu, Y., and Meyers, P. A. (2009). Sediment lipid biomarkers as recorders of the contamination and cultural eutrophication of Lake Erie, 1909-2003. *Org. Geochem.* 40 (8), 912–921. doi:10.1016/j.orggeochem.2009.04.012

McCullough, I. M., Dugan, H. A., Farrell, K. J., Morales-Williams, A. M., Ouyang, Z., Roberts, D., et al. (2018). Dynamic modeling of organic carbon fates in lake ecosystems. *Ecol. Model.* 386, 71–82. doi:10.1016/j.ecolmodel.2018.08.009

Mendonça, R., Müller, R. A., Clow, D., Verpoorter, C., Raymond, P., Tranvik, L. J., et al. (2017). Organic carbon burial in global lakes and reservoirs. *Nat. Commun.* 8 (1), 1694–1696. doi:10.1038/s41467-017-01789-6

Meng, L., Zhao, Z., Lu, L., Zhou, J., Luo, D., Fan, R., et al. (2021). Source identification of particulate organic carbon using stable isotopes and n-alkanes: Modeling and application. *Water Res.* 197, 117083. doi:10.1016/j.watres.2021.117083

Mermoud, F., Gülaçar, F. O., and Buchs, A. (1985). 5α(H)-cholestan-3α-ol in sediments: Characterization and geochemical significance. *Geochimica Cosmochimica Acta* 49 (2), 459–462. doi:10.1016/0016-7037(85)90037-7

Meyers, P. A., and Ishiwatari, R. (1993). Lacustrine organic geochemistry—An overview of indicators of organic matter sources and diagenesis in lake sediments. *Org. Geochem.* 20 (7), 867–900. doi:10.1016/0146-6380(93)90100-P

Meyers, P. A. (1997). Organic geochemical proxies of paleoceanographic, paleolimnologic, and paleoclimatic processes. *Org. Geochem.* 27 (5), 213–250. doi:10.1016/S0146-6380(97)00049-1

Middelburg, J. J. (2018). Reviews and syntheses: To the bottom of carbon processing at the seafloor. *Biogeosciences* 15 (2), 413–427. doi:10.5194/bg-15-413-2018

Naeher, S., Smittenberg, R. H., Gilli, A., Kirilova, E. P., Lotter, A. F., and Schubert, C. J. (2012). Impact of recent lake eutrophication on microbial community changes as revealed by high resolution lipid biomarkers in Rotsee (Switzerland). *Org. Geochem.* 49, 86–95. doi:10.1016/j.orggeochem.2012.05.014

Nakakuni, M., Kitano, J., Uemura, H., and Yamamoto, S. (2018). Modern sediment records of stanol to sterol ratios in Lake Suigetsu, Japan: An indicator of variable lacustrine redox conditions. *Org. Geochem.* 119, 59–71. doi:10.1016/j.orggeochem.2018.02.004

Nishimura, M., and Koyama, T. (1977). The occurrence of stanols in various living organisms and the behavior of sterols in contemporary sediments. *Geochimica Cosmochimica Acta* 41 (3), 379–385. doi:10.1016/0016-7037(77)90265-4

Niu, Y., Shen, H., Chen, J., Xie, P., Yang, X., Tao, M., et al. (2011). Phytoplankton community succession shaping bacterioplankton community composition in Lake Taihu, China. *Water Res.* 45 (14), 4169–4182. doi:10.1016/j.watres.2011.05.022

Patel, D., Gismondi, R., Alsaffar, A., and Tiquia-Arashiro, S. M. (2019). Applicability of API ZYM to capture seasonal and spatial variabilities in lake and river sediments. *Environ. Technol. (United Kingdom)* 40 (24), 3227–3239. doi:10.1080/09593330.2018.1468492

Przytulska, A., Bartosiewicz, M., and Vincent, W. F. (2017). Increased risk of cyanobacterial blooms in northern high-latitude lakes through climate warming and phosphorus enrichment. *Freshw. Biol.* 62 (12), 1986–1996. doi:10.1111/fwb.13043

Qin, B., Gao, G., Zhu, G., Zhang, Y., Song, Y., Tang, X., et al. (2013). Lake eutrophication and its ecosystem response. *Chin. Sci. Bull.* 58 (9), 961–970. doi:10.1007/s11434-012-5560-x

Qin, B., Xu, P., Wu, Q., Luo, L., and Zhang, Y. (2007). Environmental issues of Lake Taihu, China. *Hydrobiologia* 581 (1), 3–14. doi:10.1007/s10750-006-0521-5

Raymond, P. A., and Bauer, J. E. (2001). Use of ^{14}C and ^{13}C natural abundances for evaluating riverine, estuarine, and coastal doc and POC sources and cycling: A review and synthesis. *Org. Geochem.* 32 (4), 469–485. doi:10.1016/S0146-6380(00)00190-X

Robinson, N., Eglinton, G., Brassell, S. C., and Cranwell, P. A. (1984). Dinoflagellate origin for sedimentary 4α-methylsteroids and 5α(H)-stanols. *Nature* 308 (5958), 439–442. doi:10.1038/308439a0

Salk, K. R., Venkiteswaran, J. J., Couture, R. M., Higgins, S. N., Paterson, M. J., and Schiff, S. L. (2022). Warming combined with experimental eutrophication intensifies lake phytoplankton blooms. *Limnol. Oceanogr.* 67 (1), 147–158. doi:10.1002/lno.11982

Shan, K., Song, L., Chen, W., Li, L., Liu, L., Wu, Y., et al. (2019). Analysis of environmental drivers influencing interspecific variations and associations among bloom-forming cyanobacteria in large, shallow eutrophic lakes. *Harmful Algae* 84, 84–94. doi:10.1016/j.hal.2019.02.002

Sobek, S., Durisch-Kaiser, E., Zurbrügg, R., Wongfun, N., Wessels, M., Pasche, N., et al. (2009). Organic carbon burial efficiency in lake sediments controlled by oxygen exposure time and sediment source. *Limnol. Oceanogr.* 54 (6), 2243–2254. doi:10.4319/lo.2009.54.6.2243

Su, X., Steinman, A. D., Xue, Q., Zhao, Y., Tang, X., and Xie, L. (2017). Temporal patterns of phyto- and bacterioplankton and their relationships with environmental factors in Lake Taihu, China. *Chemosphere* 184, 299–308. doi:10.1016/j.chemosphere.2017.06.003

Sun, D., He, Y., Wu, J., Liu, W., and Sun, Y. (2019). Hydrological and ecological controls on autochthonous carbonate deposition in lake systems: A case study from lake wuliangsu and the global perspective. *Geophys. Res. Lett.* 46 (12), 6583–6593. doi:10.1029/2019GL082224

Tabuchi, K., Kojima, H., and Fukui, M. (2010). Seasonal changes in organic matter mineralization in a sublittoral sediment and temperature-driven decoupling of key processes. *Microb. Ecol.* 60 (3), 551–560. doi:10.1007/s00248-010-9659-9

Tang, C., Li, Y., He, C., and Acharya, K. (2020). Dynamic behavior of sediment resuspension and nutrients release in the shallow and wind-exposed Meiliang Bay of Lake Taihu. *Sci. Total Environ.* 708, 135131. doi:10.1016/j.scitotenv.2019.135131

Tranvik, L. J., Downing, J. A., Cotner, J. B., Loiselle, S. A., Striegl, R. G., Ballatore, T. J., et al. (2009). Lakes and reservoirs as regulators of carbon cycling and climate. *Limnol. Oceanogr.* 54 (62), 2298–2314. doi:10.4319/lo.2009.54.6_part_2.2298

Vachon, D., Sponseller, R. A., and Karlsson, J. (2021). Integrating carbon emission, accumulation and transport in inland waters to understand their role in the global carbon cycle. *Glob. Change Biol.* 27 (4), 719–727. doi:10.1111/gcb.15448

Visser, P. M., Verspagen, J. M. H., Sandrini, G., Stal, L. J., Matthijs, H. C. P., Davis, T. W., et al. (2016). How rising CO_2 and global warming may stimulate harmful cyanobacterial blooms. *Harmful Algae* 54, 145–159. doi:10.1016/j.hal.2015.12.006

Volkman, J. K. (1986). A review of sterol markers for marine and terrigenous organic matter. *Org. Geochem.* 9 (2), 83–99. doi:10.1016/0146-6380(86)90089-6

Volkman, J. K., Barrett, S. M., Blackburn, S. I., Mansour, M. P., Sikes, E. L., and Gelin, F. (1998). Microalgal biomarkers: A review of recent research developments. *Org. Geochem.* 29 (5–7), 1163–1179. doi:10.1016/S0146-6380(98)00062-X

Volkman, J. K. (2005). Sterols and other triterpenoids: Source specificity and evolution of biosynthetic pathways. *Org. Geochem.* 36 (2), 139–159. doi:10.1016/j.orggeochem.2004.06.013

Wagner, C., and Adrian, R. (2009). Cyanobacteria dominance: Quantifying the effects of climate change. *Limnol. Oceanogr.* 54 (62), 2460–2468. doi:10.4319/lo.2009.54.6_part_2.2460

Wang, H., Hu, X., Wetz, M. S., and Hayes, K. C. (2018). Oxygen consumption and organic matter remineralization in two subtropical, eutrophic coastal embayments. *Environ. Sci. Technol.* 52 (22), 13004–13014. doi:10.1021/acs.est.8b02971

Wang, S., Gao, Y., Jia, J., Lu, Y., Sun, K., Ha, X., et al. (2022). Vertically stratified water source characteristics and associated driving mechanisms of particulate organic carbon in a large floodplain lake system. *Water Res.* 209, 117963. doi:10.1016/j.watres.2021.117963

Watanabe, K., and Kuwae, T. (2015). How organic carbon derived from multiple sources contributes to carbon sequestration processes in a shallow coastal system? *Glob. Change Biol.* 21 (7), 2612–2623. doi:10.1111/gcb.12924

Wei, L., Cai, P., Shi, X., Cai, W. J., Liu, W., Hong, Q., et al. (2022). Winter mixing accelerates decomposition of sedimentary organic carbon in seasonally hypoxic coastal seas. *Geochimica Cosmochimica Acta* 317, 457–471. doi:10.1016/j.gca.2021.11.003

Xiao, Q., Duan, H., Qi, T., Hu, Z., Lee, X., Zhang, M., et al. (2020a). Environmental investments decreased partial pressure of CO_2 in a small eutrophic urban lake: Evidence from long-term measurements. *Environ. Pollut.* 263, 114433. doi:10.1016/j.envpol.2020.114433

Xiao, Q., Duan, H., Qin, B., Hu, Z., Zhang, M., Qi, T., et al. (2022). Eutrophication and temperature drive large variability in carbon dioxide from China's Lake Taihu. *Limnol. Oceanogr.* 67 (2), 379–391. doi:10.1002/lno.11998

Xiao, Q., Xu, X., Duan, H., Qi, T., Qin, B., Lee, X., et al. (2020b). Eutrophic Lake Taihu as a significant CO_2 source during 2000–2015. *Water Res.* 170, 115331. doi:10.1016/j.watres.2019.115331

Xu, J., Lei, S., Bi, S., Li, Y., Lyu, H., Xu, J., et al. (2020). Tracking spatio-temporal dynamics of POC sources in eutrophic lakes by remote sensing. *Water Res.* 168, 115162. doi:10.1016/j.watres.2019.115162

Xu, J., Lyu, H., Xu, X., Li, Y., Li, Z., Lei, S., et al. (2019). Dual stable isotope tracing the source and composition of POM during algae blooms in a large and shallow eutrophic lake: All contributions from algae? *Ecol. Indic.* 102, 599–607. doi:10.1016/j.ecolind.2019.03.014

Xu, X., Li, W., Fujibayashi, M., Nomura, M., Nishimura, O., and Li, X. (2015a). Asymmetric response of sedimentary pool to surface water in organics from a shallow hypereutrophic lake: The role of animal consumption and microbial utilization. *Ecol. Indic.* 58, 346–355. doi:10.1016/j.ecolind.2015.06.009

Xu, X., Li, W., Fujibayashi, M., Nomura, M., Nishimura, O., and Li, X. (2015b). Predominance of terrestrial organic matter in sediments from a cyanobacteria-blooming hypereutrophic lake. *Ecol. Indic.* 50, 35–43. doi:10.1016/j.ecolind.2014.10.020

Yan, X., Xu, X., Ji, M., Zhang, Z., Wang, M., Wu, S., et al. (2019). Cyanobacteria blooms: A neglected facilitator of CH_4 production in eutrophic lakes. *Sci. Total Environ.* 651, 466–474. doi:10.1016/j.scitotenv.2018.09.197

Yang, H., Xing, Y., Xie, P., Ni, L., and Rong, K. (2008). Carbon source/sink function of a subtropical, eutrophic lake determined from an overall mass balance and a gas exchange and carbon burial balance. *Environ. Pollut.* 151 (3), 559–568. doi:10.1016/j.envpol.2007.04.006

Zhang, F., Yao, S., Xue, B., Lu, X., and Gui, Z. (2017b). Organic carbon burial in Chinese lakes over the past 150 years. *Quat. Int.* 438, 94–103. doi:10.1016/j.quaint.2017.03.047

Zhang, Y., Peng, T., Su, Y., Yu, J., and Liu, Z. (2021). Spatial heterogeneity in fatty acid abundance and composition across surface sediments of Lake Taihu, Eastern China: Implications for the use of lipids in evaluating carbon cycling and burial in lake systems. *Catena* 201, 105225. doi:10.1016/j.catena.2021.105225

Zhang, Y., Su, Y., Liu, Z., Du, Y., Yu, J., and Jin, M. (2019). Fatty acid and alcohol compositions in lacustrine sediments as indicators of environment and ecosystem of lakes in Eastern China. *Ecol. Indic.* 97, 290–300. doi:10.1016/j.ecolind.2018.10.029

Zhang, Y., Su, Y., Liu, Z., Yu, J., and Jin, M. (2017a). Lipid biomarker evidence for determining the origin and distribution of organic matter in surface sediments of Lake Taihu, Eastern China. *Ecol. Indic.* 77, 397–408. doi:10.1016/j.ecolind.2017.02.031

Zhao, X., Yang, L., Yu, Z., Fan, Q., Zhong, Z., Xiao, Y., et al. (2007). Temporal and spatial distribution of pbysirnchemical characteristics and nutrients in sediments of Lake Taihu. *J. Lake Sci.* 19 (6), 698–704. doi:10.18307/2007.0612

Zhu, C., Zhang, J., Nawaz, M. Z., Mahboob, S., Al-Ghanim, K. A., Khan, I. A., et al. (2019). Seasonal succession and spatial distribution of bacterial community structure in a eutrophic freshwater Lake, Lake Taihu. *Sci. Total Environ.* 669, 29–40. doi:10.1016/j.scitotenv.2019.03.087